Explicit Guidance of Drag-Modulated Aeroassisted Transfer Between Elliptical Orbits

Nguyen X. Vinh* and Jennie R. Johannesen†
The University of Michigan, Ann Arbor, Michigan

Kenneth D. Mease‡
Jet Propulsion Laboratory, California Institute of Technology, Pasadena, California

and

John M. Hanson§
Analytic Services Inc., Arlington, Virginia

This paper presents the complete analysis of the problem of minimum-fuel aeroassisted transfer between coplanar elliptical orbits in the case where the orientation of the final orbit is free for selection in the optimization process. A comparison is made between the optimal pure-propulsive transfer and the idealized aeroassisted transfer, involving several passages through the atmosphere. In the case where aeroassisted transfer provides fuel savings, a practical scheme for its realization by one passage is proposed. The orbit transfer consists of three phases: A deorbit phase resulting in nonzero entry angle, followed by an atmospheric fly-through with variable drag control, and completed by a post atmospheric phase. An explicit guidance formula for drag control is derived, and it is shown that the required exit speed for ascent to final orbit can be obtained with a very high degree of accuracy.

Introduction

THE problem of minimum-fuel aeroassisted transfer between orbits has received considerable attention in recent years. The case of transfer between coplanar circular orbits has been analyzed in the literature.[1-3] In this paper, the case where the initial and final orbits are elliptical is considered. More specifically, it is proposed to transfer, with minimum-fuel consumption, a vehicle from an initial elliptical orbit O_1 to a coplanar final elliptical orbit O_2. The two Keplerian orbits are about a spherical planet with the center of attraction located at point F (Fig. 1). The orbits are defined by the apocenter and pericenter distances A_i and P_i, respectively. We shall assume that the orientation of the line of apsides is free for selection in the optimization process. This means that the argument of the pericenter of the final orbit is not important in the intended mission.

For a high-thrust propulsion system, it is assumed that the time interval for powered flight is short as compared to the orbital period. Hence, the velocity changes upon the application of the thrust can be considered instantaneous.

Idealized Optimal Transfers

We first consider the various optimal pure-propulsive transfers and select the best for comparison with the most advantageous aeroassisted transfer of an idealized sort. This is intended to display explicitly the circumstances under which aeroassisted transfer is a fuel-saving mode. In the following sections, an analysis of its practical realization is presented.

For a pure-propulsive transfer, since the orientation of the final orbit is free, in the optimal configuration the initial and

final orbits are coaxial with pericenters on the same side of the attracting center F.[4-6] For a finite-time transfer, the optimal mode is the Hohmann transfer connecting the higher apocenter to the pericenter of the other orbit. The case where the apocenter of the initial orbit is higher shall be considered, i.e., $A_1 \geq A_2$, and the dimensionless lengths and characteristic velocities conveniently defined:

$$\alpha_i = \frac{A_i}{R}, \quad \beta_i = \frac{P_i}{R}, \quad v = \frac{V}{\sqrt{\mu/R}}, \quad \Delta v_i = \frac{\Delta V_i}{\sqrt{\mu/R}} \quad (1)$$

where μ is the gravitational constant of the planet and R the radius of its surrounding atmosphere. The characteristic velocity of the Hohmann transfer, normalized with respect to the circular speed at distance R, $V_c = \sqrt{\mu/R}$, is

$$\Delta v_H = \frac{\Delta V_H}{V_c} = \left| \sqrt{\frac{2\beta_1}{\alpha_1(\alpha_1 + \beta_1)}} - \sqrt{\frac{2\beta_2}{\alpha_1(\alpha_1 + \beta_2)}} \right|$$

$$+ \sqrt{\frac{2\alpha_1}{\beta_2(\alpha_1 + \beta_2)}} - \sqrt{\frac{2\alpha_2}{\beta_2(\alpha_2 + \beta_2)}} \quad (2)$$

If $\alpha_1 \rightarrow \infty$, the initial approaching orbit is parabolic and the first impulse applied at infinity or in practice at a large distance is negligible. This leads to conceiving a parabolic transfer, even in the case where α_1 is finite. The first accelerative impulse is applied at the pericenter of the first orbit to propel the vehicle into a parabola. At infinity, upon the application of an infinitesimal impulse, the vehicle returns by another parabola with the same pericenter as in the final orbit. Another decelerative impulse is applied at this center to complete the transfer. All of the impulses are tangential; the total cost for this parabolic mode is

$$\Delta v_p = \sqrt{\frac{2}{\beta_1}} - \sqrt{\frac{2\alpha_1}{\beta_1(\alpha_1 + \beta_1)}} + \sqrt{\frac{2}{\beta_2}} - \sqrt{\frac{2\alpha_2}{\beta_2(\alpha_2 + \beta_2)}}$$

$$(3)$$

Upon direct comparison of the characteristic velocities, one can select the optimal pure-propulsive mode.

For aeroassisted transfer, a decelerative impulse is applied tangentially at the apocenter of initial orbit to lower the pericenter to the top of the atmosphere. Its magnitude is

$$\Delta v_1 = \sqrt{\frac{2\beta_1}{\alpha_1(\alpha_1 + \beta_1)}} - \sqrt{\frac{2}{\alpha_1(\alpha_1 + 1)}} \qquad (4)$$

Near the top of the atmosphere, in the vicinity of the pericenter, atmospheric drag will work to reduce the apocenter to the distance A_2 where an accelerative impulse is applied to propel the vehicle into final orbit. Its magnitude is

$$\Delta v_2 = \sqrt{\frac{2\beta_2}{\alpha_2(\alpha_2 + \beta_2)}} - \sqrt{\frac{2}{\alpha_2(\alpha_2 + 1)}} \qquad (5)$$

The total cost for this aeroassisted-elliptic mode is

$$\Delta v_{AE} = \Delta v_1 + \Delta v_2 \qquad (6)$$

and it has to be compared with the best pure-propulsive mode for optimality. Another way to bring the pericenter to the top of the atmosphere for the atmospheric decay process is to first send the vehicle into a parabolic orbit by a tangential and accelerative impulse applied at the pericenter of the initial orbit. Its magnitude is

$$\overline{\Delta v_1} = \sqrt{\frac{2}{\beta_1}} - \sqrt{\frac{2\alpha_1}{\beta_1(\alpha_1 + \beta_1)}} \qquad (7)$$

Then, at a large distance the vehicle can return on a grazing trajectory with a negligible impulse. The subsequent process of orbit decay and injection into the final orbit is as before, and for this aeroassisted-parabolic mode

$$\Delta v_{AP} = \overline{\Delta v_1} + \Delta v_2 \qquad (8)$$

By comparing Eqs. (4) and (7), it is deduced that for the two aeroassisted modes, the parabolic mode is more economical if

$$\beta_1 \geq [4(\alpha_1 + 1)]/\alpha_1 \qquad (9)$$

The aeroassisted transfer discussed in this section is based on an idealized scheme. It will require many passages through the atmosphere for A_1 to decrease to A_2. Furthermore, based on the theory of orbit contraction, it is assumed that during the decay process the pericenter is nearly stationary.[7] If this mode is optimal, the characteristic velocity computed is the idealized absolute minimum.

Practical Aeroassisted Transfer

In practice, the reduction of the apocenter occurs in a single passage. This requires a nonzero entry angle γ_e and an exit angle γ_f. The resulting total cost will be slightly higher than the idealized case.

The aeroassisted transfer consists of three phases:

The first phase is the deorbit phase. A propulsive maneuver is affected such that the vehicle enters the atmosphere at distance R at a certain prescribed angle γ_e. This very small angle is selected such that within the drag capability of the vehicle, the necessary speed depletion can be accomplished in one passage.

The second phase is the atmospheric fly-through phase. It shall be assumed that the ballistic coefficient of the vehicle can be modulated between its maximum and minimum values. By proper modulation of this coefficient, it is proposed to bring the vehicle to the best atmospheric exit condition for the vehicle to climb to the final apocenter for orbit insertion.

The third and final phase is the postatmospheric maneuver to put the vehicle into final orbit.

It will be shown in a synthesis study that all three phases are coupled; i.e. the initial entry angle is selected based on the final orbit configuration and the drag capability of the vehicle during atmospheric passage. However, in terms of fuel consumption, since the entry and exit angles are small, it is possible to analyze the optimal maneuver for each phase separately. It will be shown that the resulting characteristic velocity for the combined maneuver is very close to the idealized minimum.

Entry at Prescribed Angle

In the deorbit phase, it is proposed to find the optimal descending trajectory which intersects the atmosphere at distance R at a nonzero prescribed angle γ_e. This can be achieved by applying a single, tangential and decelerative impulse at the apocenter of the initial orbit. From the geometry of the deorbit as shown in Fig. 2, the characteristic velocity of this one-impulse mode is

$$\Delta v_I = \sqrt{\frac{2\beta_1}{\alpha_1(\alpha_1 + \beta_1)}} - \sqrt{\frac{2(\alpha_1 - 1)}{\alpha_1(\alpha_1^2 - \cos^2\gamma_e)}} \cos\gamma_e \qquad (10)$$

The cost for deorbit increases as the entry angle increases.

Another alternative is to use parabolic orbits for deorbiting. In this case, an accelerative impulse is applied tangentially at the pericenter to send the vehicle into a parabola. Then, at infinity, the vehicle can be returned along another parabola for entry at any prescribed angle with an infinitesimal impulse. The cost for this transfer is given in Eq. (7). By comparing Eq. (7) with Eq. (10) we have the explicit condition for the parabolic mode to be better than the one-impulse mode.
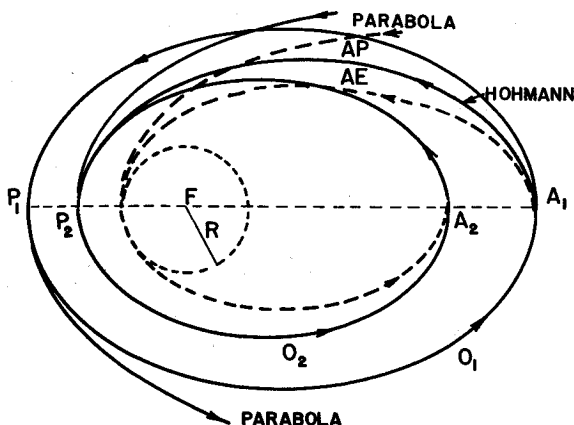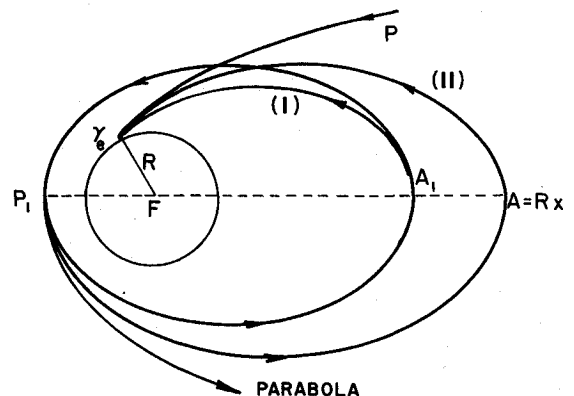

Fig. 1 Transfers between coaxial orbits.

Fig. 2 Deorbit for prescribed entry angle.

$$\beta_1 \geq \frac{4(\alpha_1 - 1)(\alpha_1^2 - \cos^2\gamma_e)\cos^2\gamma_e}{\alpha_1(\alpha_1 - \cos^2\gamma_e)^2} \qquad (11)$$

For a nonzero entry angle, there exists the possibility of the two-impulse mode as the optimal process. In this case, the first and accelerative impulse is applied tangentially at the pericenter of the initial orbit to bring the apocenter to the distance $A = Rd$. At the new apocenter, a second tangential and decelerative impulse is applied to return the vehicle for intersection at the prescribed angle. By minimizing the total characteristic velocity with respect to d, we have an equation for calculating this unknown.

In practical application the one-impulse deorbit is the preferred mode, especially in the case where the time of transfer is a critical constraint.

Explicit Guidance for Drag Modulation

The atmospheric phase in the aeroassisted maneuver is considered in this section. To begin this phase, the vehicle enters the atmosphere at distance R with a speed V_e and entry angle γ_e. The atmospheric maneuver uses lift or drag modulation to bring the vehicle to exit at $\gamma_f \approx 0$, with a resulting exit speed V_f such that the apocenter of the ascending trajectory coincides with the apocenter of the final orbit (Fig. 3). In this way, the final impulse is minimized.

The case where it is possible to modulate the ballistic drag coefficient between a lower and an upper limit is now considered. Using standard notation, the equations for ballistic flight inside a nonrotating planetary atmosphere are as follows:

$$\frac{dr}{dt} = V\sin\gamma$$

$$\frac{dV}{dt} = -\frac{\rho SC_D V^2}{2m} - g\sin\gamma$$

$$V\frac{d\gamma}{dt} = \left(\frac{V^2}{r} - g\right)\cos\gamma \qquad (12)$$

Since the flight-path angle stays small (a few degrees), the small gravity component $g\sin\gamma$ as compared to the acceleration due to the drag can be be neglected. Furthermore, the following approximations are used

$$\sin\gamma \approx \gamma, \quad \cos\gamma \approx 1, \quad g(r) \approx g(R), \quad \frac{V^2}{r} \approx \frac{V^2}{R} \qquad (13)$$

These approximations induce an error of the same order as the error committed by neglecting the Coriolis force. It should be mentioned that the assumptions used are not necessary for
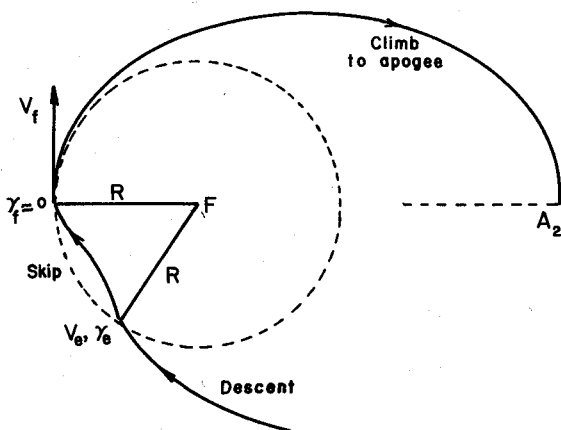

Fig. 3   Aeroassisted transfer.

the present analysis, but they have the advantage of displaying explicitly the various effects of the drag coefficient, entry speed, and entry angle on the ballistic fly-through trajectory.[8]

The density ρ is used as the altitude variable and it is assumed that this density is locally exponential, i.e.,

$$\frac{d\rho}{\rho} = -\frac{dr}{H} \qquad (14)$$

where the scale height H can be adjusted for concordance with the standard atmosphere at the altitude range of the flight. Then, with the simplification of Eq. (13) and by using the dimensionless variables

$$y = \frac{\rho}{\rho_e}, \quad \Phi = -\sqrt{\frac{R}{H}}\,\gamma, \quad x = \log\left(\frac{V_e}{V}\right)^2, \quad \theta = \sqrt{\frac{g}{H}}\,t \qquad (15)$$

and the parameters

$$\delta = \frac{gR}{V_e^2}, \qquad \epsilon = \frac{\rho_e SC_D\sqrt{HR}}{m} \qquad (16)$$

we have the equations of motion in dimensionless form:

$$\frac{dy}{dx} = \frac{\Phi}{\epsilon}, \qquad \frac{d\Phi}{dx} = \frac{(\delta e^x - 1)}{\epsilon y} \qquad (17)$$

and

$$\frac{d\theta}{dx} = \frac{\sqrt{\delta}\,e^{x/2}}{\epsilon y} \qquad (18)$$

Note that the last equation, denoting the variation of time, is decoupled from the others. The constant δ represents the effect of the entry speed with $\delta = 1$ for circular entry and $\delta = 0.5$ for parabolic entry. The parameter ϵ is the drag control parameter, subject to the constraint

$$\epsilon_{\min} \leq \epsilon \leq \epsilon_{\max} \qquad (19)$$

In this way, the design of drag control is more general since it is not restricted to the variation of the drag coefficient C_D alone. It is simply assumed that the dimensionless drag parameter ϵ, as defined in Eq. (16), can be configured to vary between two limits. The speed variable x is such that, at the initial time, $x = 0$ and is increasing monotonically. The altitude y is such that initially $y = 1$ and then increases as the altitude decreases. At exit, $y_f = 1$. In the definition of the flight-path-angle variable Φ, the ratio R/H can be taken as 900 for the Earth's atmosphere.

From the definition [Eq. (15)] of the dimensionless variables, we have at the initial time

$$\theta = 0, \quad x = 0, \quad y_e = 1, \quad \Phi_e = -\sqrt{R/H}\,\gamma_e > 0 \qquad (20)$$

It is proposed to use the drag control ϵ, subject to constraint (19), to bring the vehicle to exit at

$$x = x_f, \quad y_f = 1, \quad \Phi_f = -\sqrt{R/H}\,\gamma_f \qquad (21)$$

such that
1) The apocenter distance of the ascending orbit is A_2.
2) The speed at apocenter is maximized.

The first condition is expressed as the constraint

$$v_f^2(\alpha_2^2 - \cos^2\gamma_f) = 2\alpha_2(\alpha_2 - 1) \qquad (22)$$

where, in terms of the speed variable x, we have

$$v_f^2 = (1/\delta)e^{-x_f} \qquad (23)$$

The second condition leads to maximization of the performance index

$$J = v_a^2 = v_f^2 + \frac{2}{\alpha_2} - 2 = \frac{2(\alpha_2 - 1)\cos^2\gamma_f}{\alpha_2(\alpha_2^2 - \cos^2\gamma_f)} \quad (24)$$

Since $\alpha_2 = A_2/R$ is prescribed, this amounts to maximizing the final exit speed satisfying condition (22). From this condition, it can be seen that the best exit speed is obtained when $\gamma_f = 0$, if this can be achieved. The resulting maximized exit speed is

$$v_f = \sqrt{2\alpha_2/(\alpha_2 + 1)} \quad (25)$$

For the case of drag modulation, a grazing exit for a climb to apocenter is not possible,[8] and the optimal strategy consists of bang-bang control to achieve condition (22) with the smallest exit angle.[1] This control strategy is difficult to realize in practice since the switching time has to be very accurate—to within a fraction of 1 s—to avoid crashing.

As an alternative, the following drag control is proposed. First, a nominal trajectory is selected, with entry values γ_e and v_e for such that during the atmospheric phase with a high drag coefficient $\epsilon = \epsilon_1$ for descent until $\gamma = 0$, and a low drag coefficient $\epsilon = \epsilon_2$ for ascent until exit, we have a shallow exit angle and the trajectory overshoots the target apocenter. On the other hand, γ_e and v_e are selected such that a trajectory with a constant high drag coefficient $\epsilon = \epsilon_1$ undershoots the target apocenter. The nominal drag coefficients ϵ_1 and ϵ_2 are selected to be consistent with the physical constraint $\epsilon_{max} \geq \epsilon_1 > \epsilon_2 \geq \epsilon_{min}$. These conditions ensure that in the actual trajectory, by using a modulated drag coefficient, $\epsilon =$ variable, during the ascending phase we can achieve the required apocenter distance while obtaining a small exit angle.

Since it is difficult to control both γ_f and v_f to satisfy Eq. (22) identically, the proposed explicit guidance scheme aims at controlling v_f. The reason for this is that, based on Eq. (22) for a sensitivity analysis, we have for a small exit angle

$$\frac{\Delta\alpha_2}{\alpha_2} = \frac{v_f^2}{(\alpha_2 - v_f^2)}\left[(\alpha_2^2 - 1)\left(\frac{\Delta v_f}{v_f}\right) + \gamma_f(\Delta\gamma_f)\right] \quad (26)$$

The variation in the apocenter is more sensitive to the exit speed perturbation than to the exit angle perturbation.

To develop a variable drag control law, a nominal skip trajectory is considered as shown in Fig. 4. This trajectory, flown with $\epsilon = \epsilon_1$ until the bottom of the flight path, $\gamma_b = 0$, and $\epsilon = \epsilon_2$ until exit, provides an exit speed v_f^0 and a flight-path angle γ_f^0. As mentioned previously, this trajectory is designed to overshoot the terminal apocenter A_2. To have a correct distance α_2, a higher variable drag coefficient ϵ can be used during the ascent for an exit at v_f and γ_f satisfying constraint (22).

A value $\gamma_f < \gamma_f^0$ is then selected to compute the desired speed v_f from Eq. (22). The objective is to obtain a formula for a variable ϵ such that at exit a resulting speed $\bar{v}_f = v_f$ is obtained, with an exit angle $\bar{\gamma}_f$ relatively close to the correct value γ_f. In terms of the variables x and Φ, definition (15) is

Fig. 4   Nominal and controlled trajectories.

used. Based on the first of Eqs. (17), the exit speed can be predicted in the case where during the ascent, from any current position ϵ is held constant for the remainder of the trajectory, by integrating the equation until $y_f = 1$. An analytic solution is possible if an average value Φ_a is used for the flight-path-angle variable. We have

$$y - 1 = -\left[\Phi_a(x_f - x)\right]/\epsilon \quad (27)$$

For the average value Φ_a, the mean value between the current value Φ and the estimated exit value Φ_f can be used. This leads to use of the control law

$$\epsilon = -\frac{(\Phi + \Phi_f)(x_f - x)}{2(y - 1)} \quad (28)$$

where x_f is the desired final speed and Φ_f the estimated exit flight-path-angle variable. This control law is explicit since ϵ is continuously recomputed based on the current state, rather than on the deviation of the current state from a nominal current state. It remains to evaluate the estimated exit angle Φ_f. By combining the two equations (17), we have

$$\frac{dy}{y} = \frac{\Phi\,d\Phi}{(\delta e^x - 1)} \quad (29)$$

By treating $(\delta e^x - 1)$ as a constant, the affect of the variation of the speed is neglected. This is a good assumption since most of the speed depletion occurs during the descending phase at high drag coefficients. By integrating Eq. (29) from the lowest point, $y = y_b$, $\Phi = 0$, to exit $y = 1$, $x = x_f$, we have the estimated value for Φ_f:

$$\Phi_f^2 = 2(1 - \delta e^{x_f})\log y_b + k \quad (30)$$

In this equation, an additive correctional term k has been introduced to compensate for the error incurred in neglecting the effect of the speed variation. This value, k, is computed based on the nominal trajectory by using $\Phi_f = \Phi_f^0$ and $x_f = x_f^0$ in Eq. (30). The key to the efficacy of this approach is that, for the family of skip trajectories under consideration, the flight-path-angle behavior is relatively uniform: the flight-path angle is always small (a few degrees at most), and is monotonically increasing during the guided portion of the flight which starts at $\gamma = \gamma_b = 0$. Consequently, the flight-path angle is of minor importance in comparison with the speed. The connection of the guidance law with the nominal trajectory, embodied in the constant k which only affects the flight-path angle, is minimal and does little to disrupt the explicit nature of the guidance law.

This explicit drag-modulated control law has been tested numerically for several values of the entry speed ranging from parabolic entry, $\delta = 0.5$, to near-circular entry, $\delta = 0.9$, with excellent results. The characteristic values for the ballistic drag coefficients selected are

$$\epsilon_{max} = 0.0030, \; \epsilon_1 = 0.0024, \; \epsilon_2 = 0.0008, \; \epsilon_{min} = 0.0002 \quad (31)$$

We can, of course, use the values ϵ_1 and ϵ_2 at ϵ_{max} and ϵ_{min}, respectively, in constructing the nominal trajectory. The main effect of the ratio $\epsilon_{max}/\epsilon_{min}$ is in the widening of the family of trajectories which can be accurately controlled.

Typical results are shown in Tables 1 and 2. In these tables, the case of entry for a direct return from a geosynchronous orbit has been considered with $\delta = 0.577$ ($v_e = 1.316473$), $\gamma_e = -3.37$ deg. The relevant data from the nominal trajectory, $\epsilon_1 \rightarrow \epsilon_2$, are $x_f^0 = 0.33791280$ and $\gamma_f^0 = 2.36902405$ deg with the density at the bottom of the trajectory $y_b = 46.312955$. Using these data in Eq. (30), we deduce the value for the correctional constant, $k = 0.073233764$.
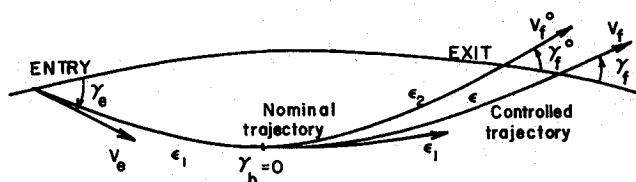
Table 1 Accuracy analysis for drag modulation using the simplified equations (17)

Dimensionless speed			Flight-path angle			Apogee distance		
Target x_f	Actual $\bar{x}_f$	Error $V_f/\bar{V}_f$	Target γ_f°	Actual $\bar{\gamma}_f^\circ$	Error $\Delta\gamma_f^\circ$	Target α_2	Actual $\bar{\alpha}_2$	Error $\Delta\alpha_2$
0.250[a]	0.265977	1.008020	2.741678	2.641190	−0.100488	2.080096	1.982009	−0.098087
0.300[a]	0.300000	1.000000	2.540464	2.507468	−0.032996	1.797377	1.797264	−0.000113
0.300[b]	0.337972	1.019167	2.540464	2.369805	−0.170659	1.797377	1.622502	−0.174875
0.350[a]	0.350000	1.000000	2.310013	2.298404	−0.011609	1.572820	1.572776	−0.000044
0.350[b]	0.359632	1.004827	2.310113	2.267438	−0.042675	1.572820	1.534810	−0.038010
0.400[a]	0.400000	1.000000	2.040099	2.063615	0.023516	1.390374	1.390477	0.000103
0.400[b]	0.400498	1.000249	2.040099	2.062626	0.022527	1.390374	1.388842	−0.001532
0.450[a]	0.450000	1.000000	1.710894	1.801546	0.090652	1.239421	1.239911	0.000490
0.450[b]	0.450000	1.000000	1.710894	1.801546	0.090652	1.239421	1.239911	0.000490
0.500[a]	0.499988	0.999994	1.276324	1.529987	0.253663	1.112755	1.114789	0.002034
0.500[b]	0.499863	0.999932	1.276324	1.530021	0.253697	1.112755	1.115067	0.002312
0.550[a]	0.500867	0.975733	0.514092	1.609839	1.095747	1.008885	1.113545	0.104660
0.550[b]	0.478900	0.965074	0.514092	1.714557	1.200465	1.008885	1.165165	0.156280

[a]$\epsilon_{max} = 0.0030$, $\epsilon_{min} = 0.0002$. [b]$\epsilon_{max} = 0.0024$, $\epsilon_{min} = 0.0008$.

Table 2 Accuracy analysis for drag modulation using the exact equations (32)

Dimensionless speed			Flight-path angle			Apogee distance		
Target x_f	Actual $\bar{x}_f$	Error $V_f/\bar{V}_f$	Target γ_f°	Actual $\bar{\gamma}_f^\circ$	Error $\Delta\gamma_f^\circ$	Target α_2	Actual $\bar{\alpha}_2$	Error $\Delta\alpha_2$
0.250[a]	0.262122	1.006079	2.748827	2.663040	−0.085787	2.080119	2.004951	−0.075167
0.300[a]	0.304179	1.002092	2.548676	2.498949	−0.049727	1.793167	1.776570	−0.016597
0.300[b]	0.333497	1.016890	2.548676	2.399986	−0.148690	1.793167	1.641670	−0.151497
0.350[a]	0.352960	1.001481	2.31770	2.292495	−0.027275	1.572857	1.560961	−0.011896
0.350[b]	0.362483	1.006261	2.319770	2.265990	−0.053780	1.572857	1.523888	−0.048969
0.400[a]	0.402204	1.001103	2.051840	2.059557	0.007717	1.390426	1.383264	−0.007162
0.400[b]	0.405271	1.002639	2.051840	2.053787	0.001947	1.390426	1.373326	−0.017100
0.450[a]	0.451464	1.000732	1.725983	1.799468	0.073485	1.239501	1.235938	−0.003563
0.450[b]	0.452615	1.001308	1.725983	1.798185	0.072202	1.239501	1.232832	−0.006669
0.500[a]	0.500538	1.000269	1.298152	1.529392	0.231240	1.112916	1.113567	0.000651
0.500[b]	0.500834	1.004171	1.298152	1.539273	0.213112	1.112916	1.12912	−0.000004
0.550[a]	0.507455	0.978952	0.570447	1.586824	1.016377	1.009869	1.099133	0.089264
0.550[b]	0.482899	0.967006	0.570447	1.708201	1.137754	1.009869	1.155509	0.145640

[a]$\epsilon_{max} = 0.0030$, $\epsilon_{min} = 0.0002$. [b]$\epsilon_{max} = 0.0024$, $\epsilon_{min} = 0.0008$.
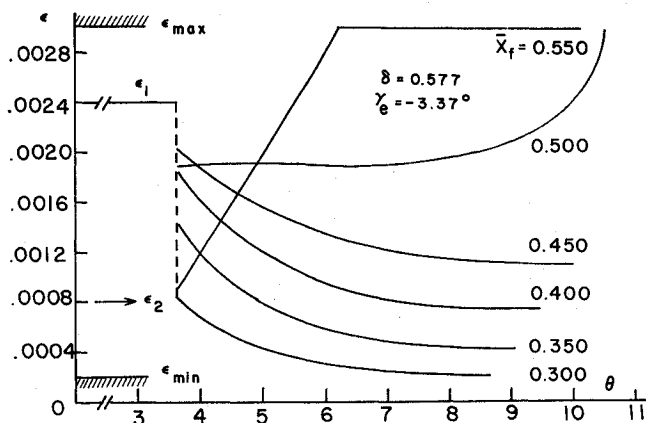

Fig. 5 Variations of the drag coefficient ϵ for various exit speeds in the case of return from geosynchronous orbit.

Table 1 presents the results from the numerical integration of the simplified equations (17) with the drag control law [Eq. (28)]. For each selected target speed x_f, the target exit angle γ_f is computed from Eq. (30). This results in a target apogee distance α_2 as computed from Eq. (22). The simplified system (17) is then integrated with ϵ_1 until the lowest point and variable ϵ until exit. The actual results are $\bar{x}_f$, $\bar{\gamma}_f$, and $\bar{\alpha}_2$. The upper lines in the table present the results for the case where ϵ_{max} and ϵ_{min} are allowed to have their extended limits as

given in Eq. (31). The lower lines in the table concern the cases where we restrict $\epsilon_{max} = \epsilon_1$ and $\epsilon_{min} = \epsilon_2$, respectively. It is clear that by narrowing the drag ratio we restrict the trajectories that can be accurately controlled to be closer to the nominal trajectory.

The variations of the drag coefficient ϵ during the controlled ascent are shown in Fig. 5. Typically, the modulated flight for ascent starts at y_b with an initial drag coefficient $\epsilon > \epsilon_2$. For high-speed exit, ϵ decreases continuously until exit, $y_f = 1$. For low-speed exit, ϵ increases to provide more speed depletion. By using a variable drag coefficient during ascent, the sensitivity problem encountered in bang-bang control is removed. Here the switching time is no longer a critical element. By using variable control, even in the case where it is not started exactly at the lowest point, it is self-corrective by using the current state to adjust the drag and, as a consequence, leads to the desired exit speed.

Table 2 presents the results from the integration of the exact equations (12). In terms of the dimensionless variables, Eqs. (12) become

$$\frac{dy}{d\theta} = -\sqrt{\frac{R/H}{\delta}}\, ye^{-x/2}\sin\gamma$$

$$\frac{dx}{d\theta} = \frac{\epsilon ye^{-x/2}}{\sqrt{\delta}} + 2\sqrt{\frac{\delta}{R/H}}\, e^{x/2}\sin\gamma$$

$$\frac{d\gamma}{d\theta} = \frac{e^{-x/2}}{\sqrt{\delta(R/H)}}(1 - \delta e^x)\cos\gamma \tag{32}$$

Since small angle simplification is no longer enforced, the drag control law has the form

$$\epsilon = \frac{\sqrt{R/H}\,(\sin\gamma + \sin\gamma_f)(x_f - x)}{2(y-1)} \qquad (33)$$

In this equation, the target exit angle is computed from

$$(R/H)\sin^2\gamma_f = 2(1 - \delta e^{x_f})\log y_b + k \qquad (34)$$

where, again, the correctional term k is evaluated using data from the nominal trajectory. For the Earth's atmosphere, the value $R/H = 900$ is used. Since the exact equations are used, the nominal trajectory with $\epsilon_1 \to \epsilon_2$ leads to the final values $x_f^0 = 0.33095987$ and $\gamma_f^0 = 2.41086279$ deg with the density at the bottom of the trajectory $y_b = 45.64071035$. From Eq. (34), it is deduced that $k = 0.08987461$. This value is used to compute the target exit angle γ_f for any target speed x_f from Eq. (34). Again, it can be seen in Table 2 that the control of the exit speed is accurate.

The variable drag control law has also been tested with a nominal trajectory obtained by using a constant average drag coefficient $\epsilon_a = (\epsilon_1 + \epsilon_2)/2$ for the entire duration of the skip. The same degree of accuracy was obtained.

Optimal Post Atmospheric Maneuver

We have seen in the previous section that at exit $\bar{v}_f$ and $\bar{\gamma}_f$ lead to an apocenter distance $\bar{\alpha}_2$. If $\bar{\alpha}_2 = \alpha_2$, a final impulse, applied tangentially at this apocenter distance, is necessary for optimal orbit insertion. The general case where $\bar{\alpha}_2 \neq \alpha_2$ is considered, and this postatmospheric phase is optimized.

The case is simple where the target apocenter $\bar{\alpha}_2 > \alpha_2$ is overshot. The final orbit is achieved by a Hohmann transfer with an accelerative impulse at $\bar{\alpha}_2$ to raise the pericenter to the level β_2 and a decelerative impulse at this center to adjust $\bar{\alpha}_2$ to the correct distance α_2.

In the case where the target apocenter is undershot, $\bar{\alpha}_2 < \alpha_2$, the first impulse Δv_1 is applied at the lowest point—the exit point—to bring $\bar{\alpha}_2$ to α_2. At this correct apocenter, a tangential and accelerative impulse Δv_2 is applied for orbit insertion. The velocity diagram at exit is shown in Fig. 6 with the Y axis along the position vector. In this system we have the components

$$\bar{X} = \bar{v}_f \cos\bar{\gamma}_f, \qquad \bar{Y} = \bar{v}_f \sin\bar{\gamma}_f \qquad (35)$$

of the exit velocity $\bar{v}$ resulting from drag-modulated fly-through and the components

$$X = v_f \cos\gamma_f, \qquad Y = v_f \sin\gamma_f \qquad (36)$$

of the correct velocity v_f required for attaining the final apocenter distance α_2. Expressed in terms of X and Y, the
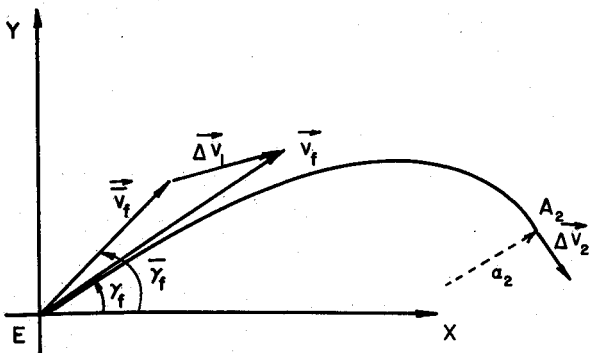

Fig. 6 Velocity diagram at exit.

constraining relations [Eq. (22)] is written as

$$(\alpha_2^2 - 1)X^2 + \alpha_2^2 Y^2 - 2\alpha_2(\alpha_2 - 1) = 0 \qquad (37)$$

Let v_2 be the speed at the apocenter in the final orbit. The sum of the two impulses Δv_1 and Δv_2 required in the post-atmospheric maneuver is

$$J = \sqrt{(X - \bar{X})^2 + (Y - \bar{Y})^2} + v_2 - (X/\alpha_2) \qquad (38)$$

Taking account of constraint (37), the Lagrange multiplier λ is introduced and the augmented function is minimized,

$$I = J + \lambda\left[(\alpha_2^2 - 1)X^2 + \alpha_2^2 Y^2 - 2\alpha_2(\alpha_2 - 1)\right] \qquad (39)$$

The necessary conditions for a stationary value of I are

$$\frac{\partial I}{\partial X} = 0, \qquad \frac{\partial I}{\partial Y} = 0 \qquad (40)$$

Upon eliminating λ between these equations and simplifying the result, we obtain

$$Y - \bar{Y} = k_1(\bar{Y}X - \bar{X}Y) \qquad (41)$$

where

$$k_1 = \sqrt{[\alpha_2(\alpha_2 + 1)]/2} \qquad (42)$$

Define the components of the first impulse, which is non-tangential

$$\Delta X = X - \bar{X}, \qquad \Delta Y = Y - \bar{Y} \qquad (43)$$

From the linear equation (41), we deduce the optimal thrust angle

$$\tan\psi = \frac{\Delta Y}{\Delta X} = \frac{k_1 \bar{Y}}{1 + k_1 \bar{X}} \qquad (44)$$

which can be immediately evaluated for given α_2, $\bar{v}_f$, and $\bar{\gamma}_f$. Let

$$k_2 = \frac{\bar{Y}}{1 + k_1 \bar{X}} \qquad (45)$$

and write Eq. (41) as

$$Y = k_2(1 + k_1 X) \qquad (46)$$

Upon substituting into Eq. (37) and solving for the positive root, the following solution is obtained:

$$X = \frac{k_1\left[2(\alpha_2 - 1)\sqrt{1 + k_1^2 k_2^2} - \alpha_2^2 k_2^2\right]}{(\alpha_2^2 - 1) + \alpha_2^2 k_1^2 k_2^2}$$

$$Y = \frac{(\alpha_2^2 - 1)k_2\left[1 + \alpha_2\sqrt{1 + k_1^2 k_2^2}\right]}{(\alpha_2^2 - 1) + \alpha_2^2 k_1^2 k_2^2} \qquad (47)$$

With this solution, the minimum characteristic velocity in post atmospheric flight is

$$\Delta v_1 + \Delta v_2 = v_2 + \sqrt{\frac{2\alpha_2}{\alpha_2 + 1}} - \sqrt{\bar{Y}^2 + \frac{(1 + k_1 \bar{X})^2}{k_1^2}} \qquad (48)$$

Hence, similar to the thrust angle, the minimum cost can be evaluated immediately in terms of α_2, $\bar{v}_f$, and $\bar{\gamma}_f$ without having to go through intermediary steps. An elegant geometric solution based on hodograph theory has been given by Marchal.[9]

Problem Synthesis

In this section, the authors shall prove the assertion that, as compared to the idealized case, which is not realistic in practice, the penalty in the fuel consumption using the present operating mode is small since the optimal condition has been realized in each phase.

The additional fuel consumption it computed first in terms of the characteristic velocity $\delta(\Delta v)$ for a nonzero entry angle γ_e, as compared to the idealized grazing entry case. The deorbit case is considered by one impulse. By comparing Eqs. (4) and (10) and linearizing for small γ_e, we have the additional characteristic velocity

$$\delta(\Delta v) = \frac{\alpha_1^2 \gamma_e^2}{2(\alpha_1^2 - 1)} \sqrt{\frac{2}{\alpha_1(\alpha_1 + 1)}} = K(\alpha_1)\gamma_e^2 \quad (49)$$

The factor $K(\alpha_1)$ is a function of the apocenter distance of the initial orbit. It is large only for $\alpha_1 \approx 1$. But, this is not the case since aeroassisted transfer is only relevant for high initial orbit. Hence, this additional characteristic velocity is small since it is of the order γ_e^2.

The additional fuel consumption for postatmospheric maneuver is due to the nonzero exit angle. This cannot be avoided due to the fact that for one-passage drag control, supercircular speed exit at zero exit angle is not possible. $\delta(\Delta v)$ is evaluated for the undershoot case. For the idealized case, a single impulse is applied at the correct apocenter with magnitude

$$\Delta v_1 = v_2 - \sqrt{2/[\alpha_2(\alpha_2 + 1)]} \quad (50)$$

On the other hand, the minimum total characteristic velocity in postatmospheric flight for the undershoot case has been given in Eq. (48). Taking the difference, we have

$$\delta(\Delta v) = \sqrt{\frac{2(\alpha_2 + 1)}{\alpha_2}} - \frac{1}{k_1}\sqrt{k_1^2 \bar{v}_f^2 + 2k_1 \bar{v}_f \cos\bar{\gamma}_f + 1} \quad (51)$$

where k_1 is defined in Eq. (42) and $\bar{v}_f$ and $\bar{\gamma}_f$ are the actual exit speed and flight-path angle resulting from the controlled atmospheric flight.

We recall that, in atmospheric flight, a small value γ_f was selected and controlled the drag to have an exit speed satisfying Eq. (22). To the order of γ_f^2, we have

$$v_f^2 = \frac{2\alpha_2(\alpha_2 - 1)}{(\alpha_2^2 - \cos^2\gamma_f)} = \frac{2\alpha_2}{\alpha_2 + 1}\left[1 - \frac{\gamma_f^2}{(\alpha_2^2 - 1)}\right] \quad (52)$$

It has been shown that this speed can be controlled accurately. Hence, in Eq. (51), we take $\bar{v}_f = v_f$ and compute

$$k_1^2 v_f^2 + 2k_1 v_f \cos\bar{\gamma}_f + 1 = (\alpha_2 + 1)^2 - \frac{\alpha_2 \gamma_f^2}{\alpha_2 - 1} - \alpha_2 \bar{\gamma}_f^2 \quad (53)$$

Since in the undershoot case $\bar{\gamma}_f < \gamma_f$, in the last equation, by taking $\bar{\gamma}_f = \gamma_f$, we have a conservative estimate of $\delta(\Delta v)$. Then, upon substituting into Eq. (51), we have

$$\delta(\Delta v) = \frac{\alpha_2^2 \gamma_f^2}{2(\alpha_2^2 - 1)} \sqrt{\frac{2}{\alpha_2(\alpha_2 + 1)}} = K(\alpha_2)\gamma_f^2 \quad (54)$$

This has the same functional form as Eq. (49), although here have the case of a small value of α_2. When $\alpha_2 \approx 1$, however, γ_f is generally very small. For example, for an Earth orbit with the entry altitude at 120 km and very low final apocenter at 380 km, we have $\alpha_2 = 6758 \text{ km}/6498 \text{ km} = 1.04$. The function K has the value $K(\alpha_2) = 6.4347$ and is still acceptable for a low exit angle.

For the overshoot case, similar analysis leads to the same order of magnitude for $\delta(\Delta v)$.

Conclusions

This paper presents a complete analysis of the problem of minimum-fuel aeroassisted transfer between coplanar elliptical orbits in the case where the orientation of the orbit is free. The optimal pure-propulsive transfer is compared with an idealized aeroassisted transfer. In the case where aeroassisted transfer is fuel-saving, its practical realization is achieved in three phases: A deorbit phase resulting in nonzero entry angle, followed by an atmospheric passage with variable drag control, and completed by a postatmospheric phase. The optimal process is discussed separately for each phase, and it is shown that the penalty in characteristic velocity, as compared to the idealized aeroassisted transfer, is of second order in the entry and exit angles. For the atmospheric phase, a drag modulation is proposed to continuously guide the vehicle to the required exit speed. An explicit control law for the drag parameter is obtained in terms of the current state of the vehicle. This control law has been tested numerically for several values of the entry speed ranging from parabolic entry to near-circular entry with excellent results.

References

[1] Kechichian, J.A., Cruz, M.I., Vinh, N.X., and Rinderle, E.A., "Optimization and Closed Loop Guidance of Drag-Modulated Aeroassisted Orbital Transfer," AIAA Paper 83-2093, Aug. 1983.

[2] Mease, K.D. and Vinh, N.X., "Minimum Fuel Aeroassisted Coplanar Orbit Transfer Using Lift Modulation," *Journal of Guidance, Control and Dynamics*, Vol. 8, Jan.-Feb. 1985, pp. 134-141.

[3] Cruz, M.I., "Trajectory Optimization and Closed Loop Guidance of Aeroassisted Orbital Transfer," AAS Paper 83-413, Aug. 1983.

[4] Marec, J.P., *Optimal Space Trajectories*, Elsevier Scientific Publishing Co., Amsterdam and New York, 1979.

[5] Marchal, C., "Synthesis of the Analytical Results on Optimal Transfers Between Keplerian Orbits (Time-free Case)," ONERA TP 482, 1967.

[6] Vinh, N.X. and Marchal, C., "Analytical Solutions of a Class of Optimum Orbit Modifications" NASA CR-1379, 1969.

[7] Longuski, J.M. and Vinh, N.X., "Analytic Theory of Orbit Contraction and Ballistic Entry into Planetary Atmospheres," JPL Pub. 80-58, 1980.

[8] Vinh, N.X., Johannesen, J.R., Longuski, J.M., and Hanson, J.M., "Second Order Analytic Solution for Aerocapture and Ballistic Fly-through Trajectories," *The Journal of the Astronautical Sciences*, Vol. 32, Oct.-Dec. 1984, pp. 429-445.

[9] Marchal, C., "Optimization de la Phase Extra-Atmosphérique de la Montée en Orbite," *La Recherche Aérospatiale*, No. 116, 1967, pp. 3-12.